

Model Behavior and the Strengths of Causal Loops: Mathematical Insights and a Practical Method

John Hayward

Division of Mathematics and Statistics, University of Glamorgan,

Pontypridd, CF37 1DL, Wales, UK

(+44)1443 654370, jhayward@glam.ac.uk

Presented at the 30th International System Dynamics Conference

St Gallen, Switzerland, 2012

Abstract

Quantifying the strength of causal loops on a stock can help bring insights into the relationship between model structure and behavior. This paper uses mathematics to derive loop strengths in a number of generic small models using the relationship between the second and first derivative from the Pathway Participation Metric method. The loop strengths are plotted in a System Dynamics (SD) simulator together with the stocks to help explain behavior in the Limits to Growth, Predator-Prey, Diffusion and SIR models among others. Issues such as loop dominance, flow dominance and the change of polarity of higher order loops are used to explain behavior. In particular the identity of the causal loops in the Diffusion and SIR models are discussed and compared with previous work. Finally a numerical method for computing loop strengths and identifying dominant loops within an SD simulator is presented and applied to the Yeast Model. It is hoped that the paper will inspire others to use loop strengths in their analysis and understanding of SD models.

Key Words: System dynamics, causal loops, SIR model, yeast model, loop dominance, pathway participation metric.

1 Introduction

1.1 Model Structure and System Dynamics

A central premise of system dynamics is that dynamical behavior can be explained by model structure. Recently Richardson (2011) characterized the field of system dynamics as:

System dynamics is the use of informal maps and formal models with computer simulation to uncover and understand endogenous sources of system behavior.

The “informal maps” include the causal loops of the more formal system dynamics model which provide a powerful and intuitive explanation of model behavior in terms of its structure. The formal system dynamics model is however more than causal loops, it consists of the *feedback loops, stocks, flows and non-linearities created by the interaction of the physical and institutional structure of the system with the decision making processes of the agents acting within it* (Sterman, 2000, p.107). Feedback loops are essential as these are key to the endogeneity of the system, the main feature that determines the power of the model to explain phenomena (Richardson, 2011). However they are not the only element that determines structure, in addition there are the stock (level) variables that represent accumulations and the flow (rate) variables that represent activity within the feedback loops (e.g. Forrester, 1968a, as quoted in Richardson, 2011).

As such, feedback loops are not sufficient to explain system behavior alone; the stocks and flows of the system need to be identified in order to capture its full structure and hence explain its full behavior. The system dynamics (SD) model is that interconnected network of entities that includes rate and accumulation relationships in addition to algebraic connections and delays. The model can be reduced to causal loop diagrams in order to explain behavior in a simple and intuitive way, but the loss of information about accumulations, and the flow structure, runs the risk of confusing and incorrect explanations (Richardson 1986; 1995; 1997). Additionally the SD model can be reduced to a set of ordinary differential equations for more a mathematical analysis. However, although this retains the stock/flow relationship in the integration, it loses some of the causal structure, which is precisely the information the system dynamicist hopes to use to explain the behavior. An SD model is more than a set of causal loops and more than a set of differential equations. Both are required to do justice to the word “structure” in the SD model.

1.2 Problems Using Causal Loops to Explain Behavior

The fact that causal loops do not capture all the structure in an SD model can lead to problems if they alone are used to interpret the model’s behavior:

1. **The presence of a stock/flow combinations in the loop.** Every causal loop must have at least one stock, and thus at least one flow. As such at least one causal link in the loop is a material (additive) one where positive polarity means “add to”, rather than an information (proportional) link, where it means “change the same way” (Richardson 1986; 1997). Whereas an information link can be reversed, a material link may not be, unless there are other processes that affect the stock. For example if x is connected to a *stock* y with positive polarity then reducing x does not reduce y but adds less to it. Thus unless there are other processes removing material from y , reducing x means y increases more slowly.
2. **The relative strengths of the causal loops.** The mere presence of a loop in a causal loop diagram does not guarantee that it is significant in explaining the behavior of the system. Loops have different strengths and some are more important than others. This has led to methods to search for dominant loops and structures (Ford, 1999; Mojtabehzadeh et.al., 2004; Kampmann & Oliva, 2011).
3. **The degree of non-linearity of a loop.** If an effect has two or more causes then the

mechanism that describes their combination may be non-linear, e.g. multiplicative. This leads to loops having variable strength and thus loop dominance will change over time. Additionally this may lead to bifurcations and a resulting change of mode (Richardson, 1995).

4. **The order of a loop.** That is the number of stocks in the loop. Although a second or higher order loop has a fixed polarity, the *effect* of the loop on an individual stock at a given time may change its polarity. For example if x and y are both stocks in a reinforcing loop with positive links, an increase in x will add more to y . But if y has other processes reducing its level at a faster rate than any of its inflows, then y will continue to decrease, albeit slower, and thus its effect on x is to slow its growth, a negative effect. Thus non-first order loops may flip their polarity on a given stock as net flows change sign. Such behavior is the source of oscillations (Richardson, 1995; Mojtahedzadeh & Richardson, 1995).
5. **Confusion over the number of loops in the system.** For example the SIR model for the spread of a disease can be constructed with two, three or more loops, but with identical behavior across the models. Although the extra loops help explain the construction of the model they do not appear to help explain its behavior (Lyneis & Lyneis, 2006).

1.3 Quantitative Approaches to Causal Loops

In the light of the problems encountered using causal loop diagrams it would be useful if the effect of the loops, and other structures, could be quantified. Kampmann & Oliva (2011) review the current state methods for structural dominance, to which the reader is referred. Briefly there are four types of methods: Traditional control theory; pathway participation metrics (e.g. Mojtahedzadeh et.al., 2004); eigenvalue elasticity analysis (e.g. Kampmann, 1996) and eigenvectors & dynamic decomposition weights (e.g. Guneralp, 2005).

In addition there are a number of behavioral methods for the detection of dominant structures such as loop deactivation (Ford, 1999; Phaff, 2008; Huang, 2009), and tracking loop gains (Kim, 1995). These have the advantage over the more formal methods in that they can be incorporated into propriety SD simulation software and do not require the use of advanced mathematical techniques or bespoke tools.

Although all the methods shed insight on the quantitative behavior of loops and structure they only give a partial description of behavior. Perhaps for this reason, and also the complexity of their application, no method is as yet in widespread use in the SD community. This is a continuing area for research.

1.4 Outline of Paper

This paper intends to shed some light on the method used in the pathway participation metric (PPM) to help relate causal loop structure to behavior. The specific aims of the paper are two-fold: To investigate mathematically causal loop strengths, incorporating them in SD simulations to help explain stock behavior; to develop a practical method of incorporating

the numerical derivation of the loop strengths in a propriety SD simulator to allow their use without the need for mathematical calculation. The purpose is to develop a method that can provide insight into the relationship between structure and behavior at different phases of a system’s history.

The method is outlined in section 2. The models are kept deliberately simple in order to widen the accessibility of the method. Additionally the models used are generic to simplify the mathematical analysis and focus on essential model structure. All the models have been implemented in Stella¹, including plots of loop strengths and the identification of loop dominance. For clarity the models and graphs in the mathematical sections (3–5) have been re-presented but all have their counterparts in Stella.

The practical method is illustrated (section 6) with the well known Yeast Model. In this section, and the associated appendix, Stella notation and graphs are retained to help the reader use the method in conjunction with the SD model.

2 Outline of Method

The behavior of any element in a system dynamics model is partly determined by the structure of the feedback loops through that element. A feedback loop must contain at least one stock, call it x . In order to obtain the effect of a particular loop on the behavior of x the question can be asked: if x increases what is the subsequent effect of that increase on x itself; does it change faster or does it change slower as a result of that initial change? The former is a reinforcing loop where there is acceleration, and the latter a balancing one, where there is retardation. Essentially this question explores the link between the change in x , i.e. the derivative, or net flow, \dot{x} , and the second derivative, or curvature, \ddot{x} . It is this relationship that underlies the pathway participation metric (PPM) method (Mojtahedzadeh et.al., 2004); Richardson’s (1995) description of loop polarity and Ford’s (1999) behavioral approach to loop dominance.

However the feedback loops are not the only type of structure that determines the behavior of the stock x , the net flow will govern whether x is increasing, decreasing, or stationary at any time. Thus the sign of \dot{x} also needs to be considered in order to understand behavior. Thus four types of “structure” can be identified: R^+ , R^- , B^+ and B^- , where the letter refers to the nature of the feedback loop and the sign refers to the net flow of x . There are four atomic behavior patterns associated with these structures: accelerating growth, accelerating decline, decelerating growth and decelerating decline (figure 1). Ford (1999) refers to the first two as exponential with an index of +1, and the latter two as logarithmic with an index of -1. The sign of \dot{x} is not indicated in the behavioral method as it concentrates on identifying dominant loops, irrespective of growth or decline. If the cases of either or both the first and second derivatives being equal to zero are considered then up to nine atomic behavior patterns can be identified (Kampmann & Oliva, 2011). As the extra cases often only occur at a critical point when a derivative is changing sign these will be omitted for simplicity.

¹Stella is produced by *isee systems*, USA. www.iseesystems.com

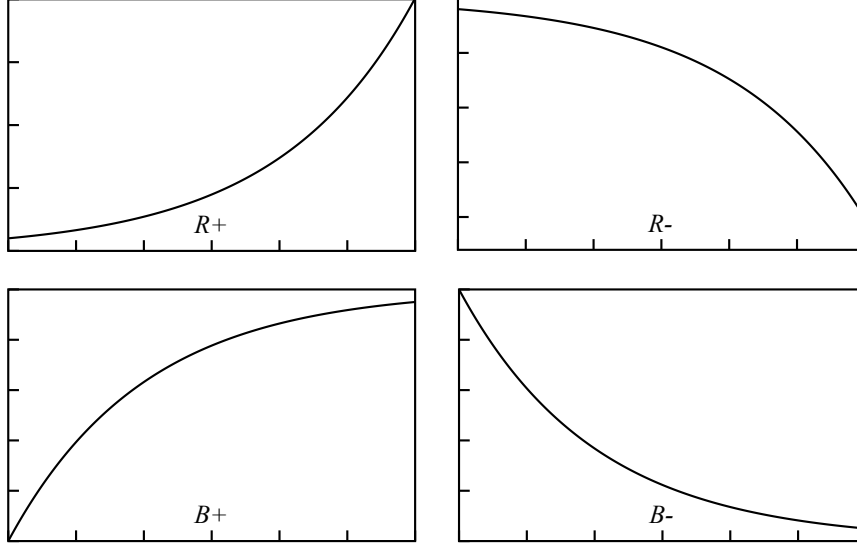


Fig. 1: Atomic Behavior Patterns Associated with Loop and Flow Structure.

For a first order autonomous system (1):

$$\dot{x} = f(x) \quad (1)$$

where $f(x)$ represents the relationships between the stock $x \geq 0$ and its flows. The relationship between the first and second derivative of x , and thus the loops, can be identified by differentiation:

$$\ddot{x} = f'(x)\dot{x} = \sum_{k=1}^m A_k \dot{x} \quad (2)$$

$f'(x)$ will identify the number m , polarity and strengths of the causal loops A_k (Richardson, 1995; Mojtahedzadeh et.al., 2004). In this definition the strength of a loop is a measure of its effect on the target stock x .

For a higher order system the situation is more complex as at least one loop will have two or more stocks and thus place a delay in the loop. For a second order system with stocks x , y :

$$\dot{x} = f(x, y) \quad (3)$$

$$\dot{y} = g(x, y) \quad (4)$$

Differentiating (3) gives the relationship between the first and second derivatives of x :

$$\ddot{x} = \frac{\partial f}{\partial x} \dot{x} + \frac{\partial f}{\partial y} \dot{y} = \frac{\partial f}{\partial x} \dot{x} + \frac{\partial f}{\partial y} \frac{dy}{dx} \dot{x} = \frac{\partial f}{\partial x} \dot{x} + \frac{\partial f}{\partial y} \frac{g}{f} \dot{x} \quad (5)$$

using the chain rules for partial and total differentiation and substituting from equations (3–4). The first term $\partial f/\partial x$ will identify the first order loops for a given f once the partial derivative is decomposed into different terms, as in (2). The second term $(\partial f/\partial y)(g/f)$ will contain the effects of the second order loops, but may also contain effects on x from y that are exogenous and not part of any of its loops. This will be explored in the examples.

Equation (5) is a special case of equation (4) in (Mojtahedzadeh et.al., 2004), the n^{th} order system. A similar equation can be identified for the effects of the loops on y .

Once the partial derivatives are decomposed into loops the different strengths of the loops on a given stock can be identified. In the PPM method a metric is defined that gives the relative strength of each loop in order to identify dominant structures. In this paper the actual values of the strengths will be derived and examined as issues other than loop dominance will be considered, such as the contrast with net flow.

3 First Order Models

3.1 Compounding and Draining Process

Consider the standard compounding and draining process, with a constant outflow, figure 2 with corresponding equation (6).

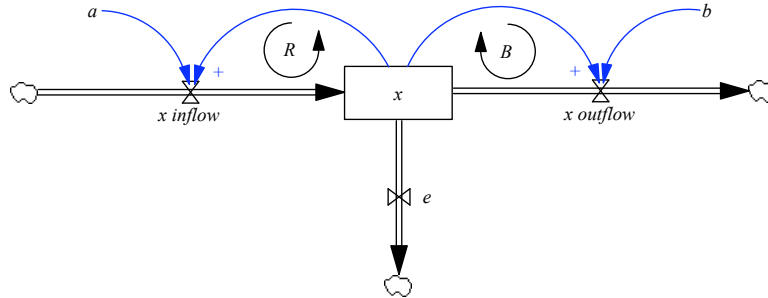


Fig. 2: Compounding and Draining Process, SD Model.

$$\dot{x} = ax - bx - e \quad (6)$$

It is assumed $x \geq 0$. The model is linear with a reinforcing loop R and balancing loop B . This model is considered first as the constant loop dominance will be a contrast to the later more complex models.

Differentiating (6) gives:

$$\ddot{x} = (a - b)\dot{x} \quad (7)$$

showing the strengths and polarity of the loops, $S(R) = a$ and $S(B) = -b$. The strengths are constant due to the linearity of the system. Thus one loop is always dominant throughout (unless $a = b$), and the behavior of the system is determined by which loop is the stronger. For example, in figure 3, $a > b$, $e = 0$, thus the reinforcing loop dominates $|S(R)| > |S(B)|$, with R^+ behavior. For $a < b$, $e = 0$ the balancing loop dominates with B^- behavior. Thus increasing b has not only changed the loop dominance but also the flow dominance of x , from growth to decline. The equilibrium point at $x_{eq} = 0$ has changed from unstable to stable.

Although the outflow e has no effect on loop dominance its value does effect the flow dominance of x . In figure 4 both curves have $a > b$ thus the reinforcing loop is dominant in both. However the dashed curve has a higher value of the constant outflow e and thus the behavior has changed from R^+ to R^- . The equilibrium point $x_{eq} = e/(a - b)$ remains unstable, thus if the initial value $x_0 > x_{eq}$ then $\dot{x} > 0$ and the behavior is R^+ , and if $x_0 < x_{eq}$ then $\dot{x} < 0$ and the behavior is R^- .

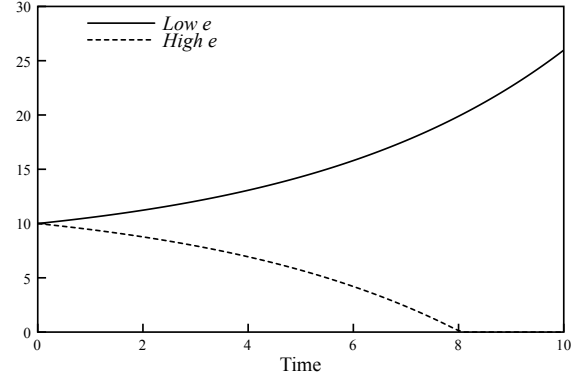
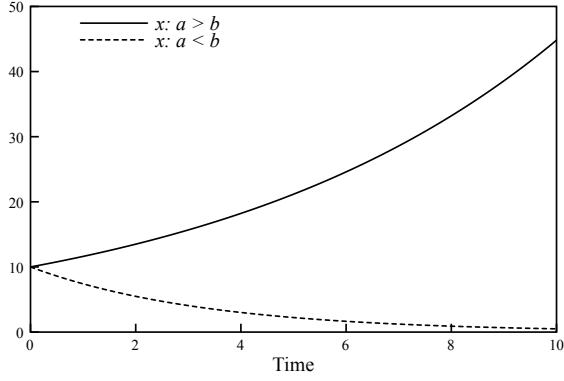


Fig. 3: Compounding & Draining Process, $e = 0$. Fig. 4: Compounding & Draining Process, $a > b$.

Thus model behavior is not only determined by the loop structure but also the flow structure, in particular the sign of the net flow. In this linear first order model the loop strengths are constant and there is a single equilibrium point thus there is no change of either flow or loop dominance throughout.

3.2 Limits to Growth

The limits to growth model (figure 5) is non-linear as the loop $B1$ acts as a slowing process on the growth rate of the reinforcing loop R . This is reflected in the term $axq = ax(1 - p) = ax(1 - x/M)$ in the equations (8). M is the capacity of the growth, however the presence of the outflow, controlled by the draining process $B2$, will ensure the growth stops before M is reached.

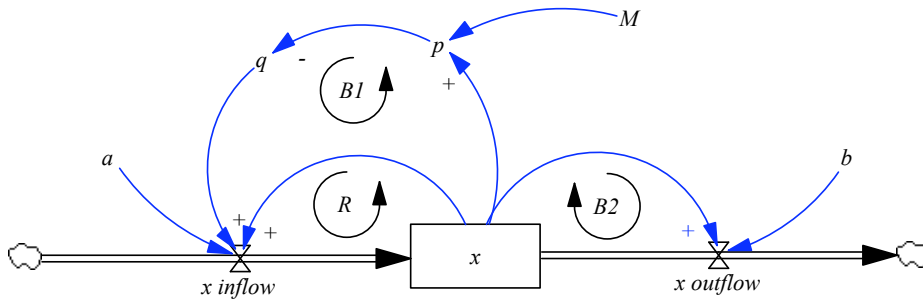


Fig. 5: Limits to Growth, SD Model.

$$\dot{x} = ax \left(1 - \frac{x}{M}\right) - bx \quad (8)$$

Setting $\dot{x} = 0$ in (8) gives the non-zero equilibrium point:

$$x_{eq} = M \left(1 - \frac{b}{a}\right) \quad (9)$$

which is stable if $a > b$, that is if there is sufficient growth compared with losses.

The strengths of the loops on the inflow will not remain constant. Differentiating (8) gives:

$$\ddot{x} = \left[a \left(1 - \frac{x}{M}\right) - \frac{a}{M}x - b \right] \dot{x} \quad (10)$$

where the structure of the model has been preserved in the differentiation of the first term. That is the product rule is used on $x(1 - x/M)$ without multiplying out the brackets. Thus (10) identifies the strengths of each loop: $S(R) = a(1 - x/M)$, $S(B1) = -ax/M$ and $S(B2) = -b$. Clearly as x increases $|S(R)|$ will decrease and $|S(B1)|$ will increase. If the system starts with R dominant then it will eventually change to the balancing loops dominating. This is shifting loop dominance, figure 6.

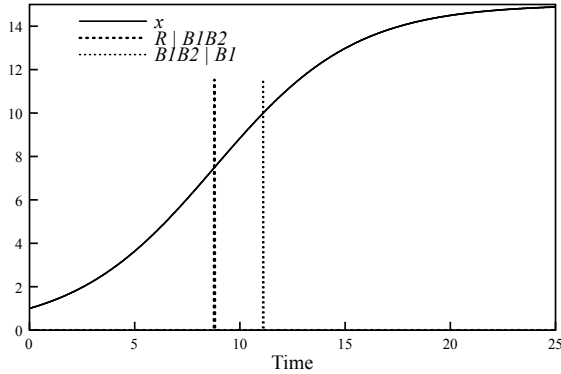


Fig. 6: Loop Dominance, Limits to Growth.

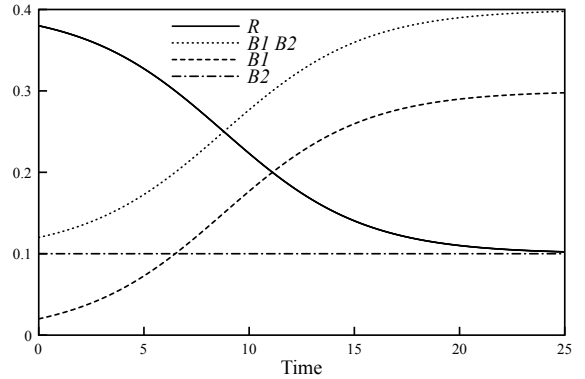


Fig. 7: Loop Strengths, Limits to Growth.

The absolute loop strengths $|S(R)|$, $|S(B1)|$ and $|S(B2)|$ can be computed and plotted within an SD simulation, figure 7. In order to identify the dominant loop or loop combination, the sum of the two balancing loops is also computed. It can be seen that there are three phases. Firstly the reinforcing loop R dominates to the point that it drops below the $B1B2$ curve. Secondly the sum of the two balancing loops dominates over R until the $B1$ curve exceeds the R curve figure 7. In this third phase $B1$ is strong enough to dominate R on its own.

The three phases can be indicated on the same graph as the plot of x , the vertical lines $R|B1B2$, $B1B2|B1$, representing the transitions, figure 6. These lines are constructed using the loop picker algorithm on the causal loop strengths (see section 6 and appendix). The transition from R to both balancing loops dominating together occurs at the inflection point.

4 Higher Order Models

4.1 Second Order Linear Model

In a second order model it is now possible for a stock to feedback on itself via another stock. Consider the system with one first order balancing loop that attempts to adjust a stock x toward a target y , with a second order reinforcing loop that causes the target y to increase as x increases, figure 8 and equations (11–12)

$$\dot{x} = a(y - x) \quad (11)$$

$$\dot{y} = cx \quad (12)$$

Differentiating (11) derives the strength of the two causal loops that affect x :

$$\ddot{x} = ay - a\dot{x} = \left(a \frac{\dot{y}}{\dot{x}} - a \right) \dot{x} = \left(\frac{cx}{y - x} - a \right) \dot{x} \quad (13)$$

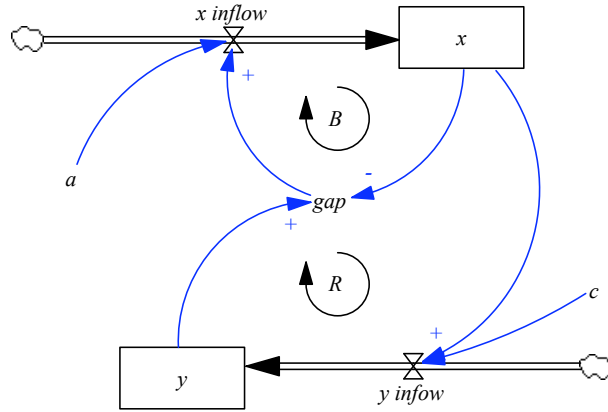


Fig. 8: 2nd Order Model.

Thus the reinforcing and balancing loop have strength:

$$S(R) = \frac{cx}{y-x} \quad (14)$$

$$S(B) = -a \quad (15)$$

where the chain rule has been used to derive the instantaneous effect of the second order loop on x , called an implicit loop by Mojtahedzadeh & Richardson (1995).

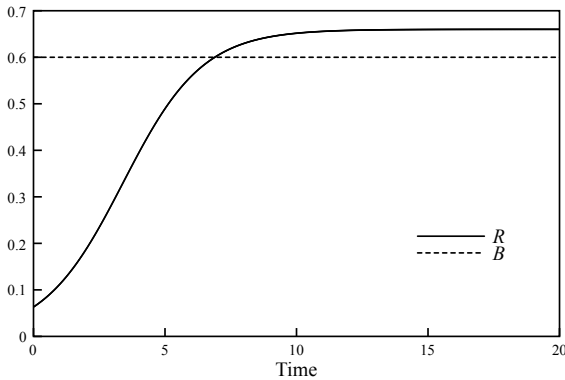


Fig. 9: Loop Strengths, 2nd Order Model.

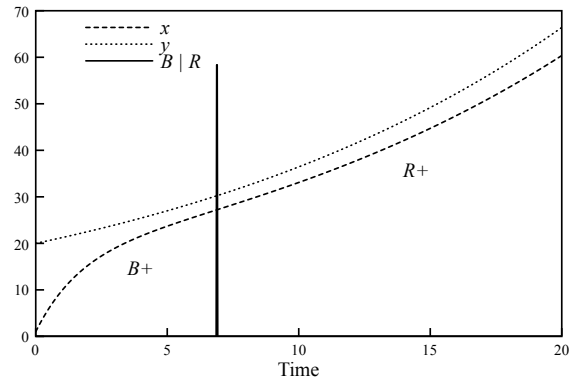


Fig. 10: Loop Dominance, 2nd Order Model.

The balancing loop is constant as it is a linear first order loop. However the reinforcing loop has a variable effect on x because it is second order and its impact is delayed. Thus there are scenarios where the constant balancing loop B dominates initially, but is eventually overtaken by the growing reinforcing loop, figure 9. Thus the behavior of x is initially B^+ , followed by R^+ as the delayed reinforcing loop dominates, figure 10. The vertical line $B|R$ marks the change of dominance. Note that y only has a reinforcing loop and is always R^+ .

To confirm the above analysis by causal loops, a stability analysis shows that the equilibrium point is a saddle instability. The solution for x is of the form $x = C_1e^{-m_1t} + C_2e^{m_2t}$, where $m_1, m_2 > 0$. If $m_1 \gg m_2$ the declining exponential dominates initially, the balancing effect, but the growing exponential always dominates ultimately. The relative values of m_1, m_2 govern the delay in the second order reinforcing loop.

With y having a similar form to x , $y = C_3e^{-m_1t} + C_4e^{m_2t}$, then as t increases, the reinforcing

loop (15) tends to a constant value:

$$S(R) = \frac{cx}{y-x} \approx \frac{cC_2e^{m_2t}}{C_2e^{m_2t} - C_4e^{m_2t}} = \frac{cC_2}{C_2 - C_4}$$

as shown in figure 9. However, although the solution has confirmed the causal loop analysis, the plots of the strengths of the loops, figure 9, are sufficient to explain the behavior, figure 10, in terms of structure.

4.2 Dominance of Non Loop Structures

Although computing the second derivative (13) has picked up the effect of the second order loop on x , strictly speaking the first term is due to the overall effect of y on x regardless of whether y is in a loop through x or not. For example, breaking the link from x to the inflow of y and replacing it by a first order reinforcing loop from y gives only one causal loop for x , (figure 11 and equations (16 –17)):

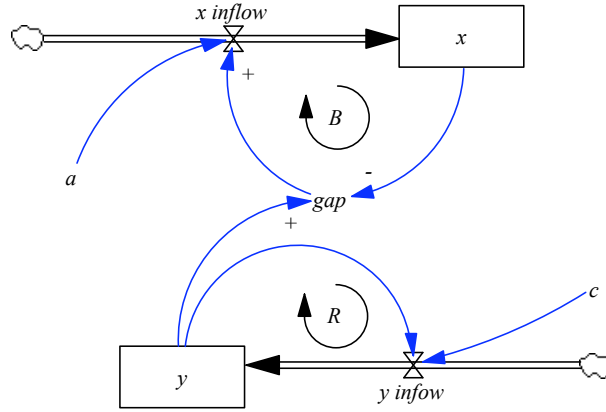


Fig. 11: Second Order Model with a Reinforcing Loop Exogenous to x .

$$\dot{x} = a(y - x) \quad (16)$$

$$\dot{y} = cy \quad (17)$$

Although there is only one loop through x there are still two terms in the curvature of x , $\ddot{x} = (cy/(y-x) - a)\dot{x}$ as the now exogenous system in y still affects x .

The resulting behavior for x is identical to the endogenous system as the reinforcing loop through y only is reflected in x . It needs to be remembered that the causal loops through a variable are not the only structures that determine behavior. In this case the curvature analysis has picked up the effect of the exogenous stock/flow structure on the stock x . Thus in this case of exogenous behavior it would be more correct to refer to *structural* dominance on x as the second phase is dominated by a reinforcing loop not through x itself, (see Kampmann & Oliva, 2011).

4.3 Oscillating Systems

Endogenous oscillation can occur when the restorative effect of a balancing loop is delayed due to the presence of extra stocks in the loop. Consider the standard Volterra predator

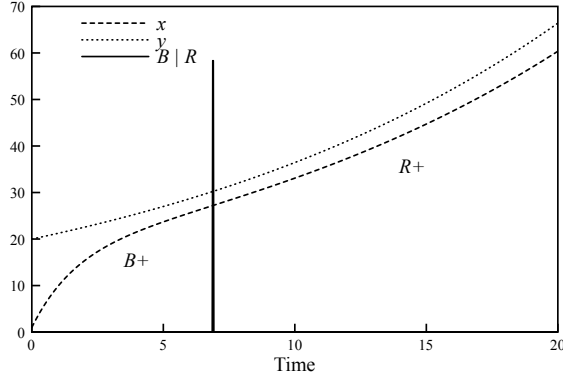


Fig. 12: Structural Dominance in a Second Order Model with a Reinforcing Loop Exogenous to x .

-prey system when x is the prey and y is the predator, figure 13 equations (18–19).

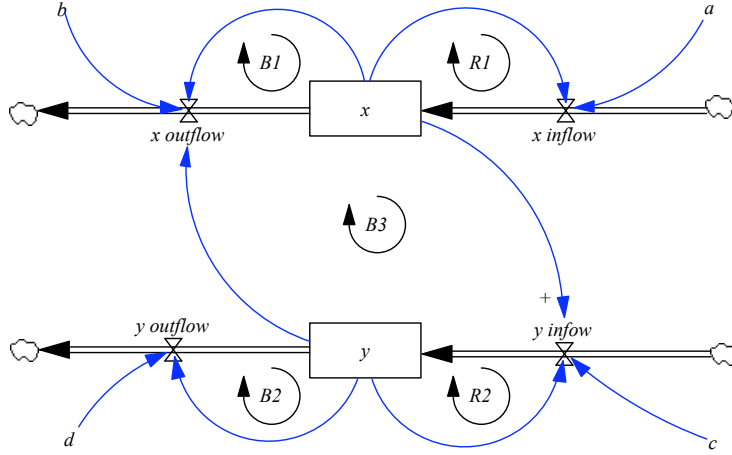


Fig. 13: Predator-Prey System, SD Model.

$$\dot{x} = ax - bxy \quad (18)$$

$$\dot{y} = cxy - dy \quad (19)$$

All the loops are first order except $B3$ which is second order. To find its instantaneous effect on the stock x , differentiate (18):

$$\begin{aligned} \ddot{x} &= a\dot{x} - bxy - by\dot{x} = \left(a - bx \frac{dy}{dx} - by \right) \dot{x} \\ &= \left(a - b \frac{y(cx - d)}{(a - by)} - by \right) \dot{x} \end{aligned} \quad (20)$$

The first and last terms are the first order loops through the prey x : $S(R1) = a$, $S(B1) = -by$. The second order balancing loop has a more complex instantaneous strength

$$S(B3) = -b \frac{y(d - cx)}{(b - ay)} \quad (21)$$

which may take both positive and negative values. Thus although it is a balancing loop the effect of its higher order is to delay the corrective action and thus induce a succession of B^- , R^+ , B^+ , R^- behavior on x , typical of an oscillation, (the curve in figure 14). The loop $B3$ has a variable polarity in terms of its effect on x , i.e. as an implicit loop (Mojtahedzadeh & Richardson, 1995). Such loops will be referred to as *flip loops* in this paper as they have the potential to flip polarity, depending on the flow dominance of x and y .

Using the loop picker algorithm (section 6 and appendix) the regions of loop dominance can be determined, showing in some regions $B3$ is having a balancing effect and may be combined with $B1$, and in other regions $B3$ is having a reinforcing effect and is sometimes combined with $R1$. Initially $B1$ dominates, figure 14, followed by $B3$, as its effect is negative (figure 15) and the x curve is B^- . $B3$ remains dominant throughout the minimum point. The curve for x becomes R^+ , as the flow dominance on x switches from negative to positive and $B3$ has a positive effect on x (figure 15). The infinity in its strength at the turning point is because at such a point $\dot{x} = 0$, thus with this definition of loop strength, the subsequent effect of a change in x on its curvature is ill defined as it is momentarily not changing². The loop is still balancing as it is still opposing the motion of x but its *immediate effect* on x is out of phase due to the delay of y and thus its sign changes, as the net flow changes sign.

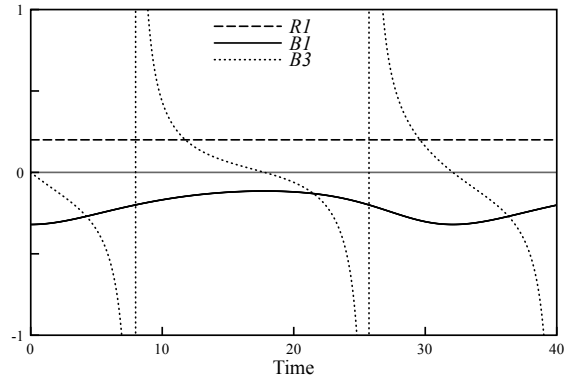
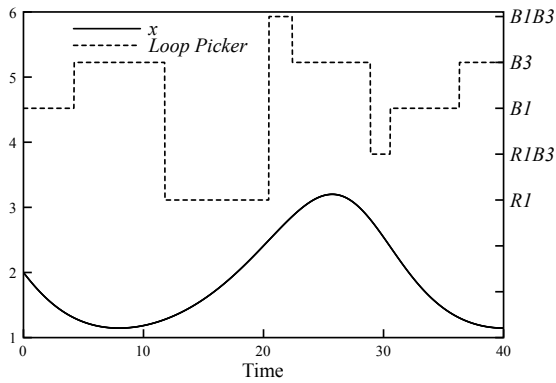


Fig. 14: Loop Dominance, Predator Prey Model. Fig. 15: Loop Strengths, Predator Prey Model.

As $B3$ weakens, $R1$ becomes dominant. At the inflection point the R^+ changes to B^- and thus the balancing loops $B1$ and $B3$ become dominant. Note that the effect of $B3$ has now gone back to negative, (figure 15). Again $B3$ is dominant around the maximum point. Indeed, in this model, the turning points are not explained by a change of loop dominance, $B3$ is dominant in both, but by a change in flow dominance on x and a reversal of the polarity of the second order loop $B3$.

It should be noted that there are phases where no single loop through x is dominating its behavior. The second order loop $B3$ is sometimes combined with either $R1$ or $B1$ for dominance to occur, depending on its polarity. That polarity is partly determined by the relative strengths of $R2$ and $B2$ and thus it would be possible to uncover the relative impact of the five loops on the system as a whole, as in Mojtahedzadeh (2009a, figure 5).

²The infinity is normalized to unity in PPM as relative loop strengths are used

5 Diffusion and Epidemic Models

5.1 Issues in Diffusion models

The loops of the Bass product diffusion model have caused some discussion as to the number, and nature, of the loops through each stock (Lyneis & Lyneis, 2006; Kampmann & Oliva, 2011). Taking the analogy of the spread of a disease let S be the susceptibles, or potential customers and I the infected, or actual customers who spread information about the product by word of mouth. At its simplest the two loop version can be described as in figure 16, equation (22–23).

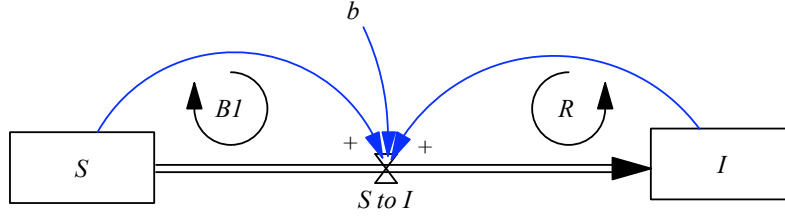


Fig. 16: Diffusion, SD Model.

$$\dot{S} = -bSI \quad (22)$$

$$\dot{I} = bSI \quad (23)$$

Considering the loops through I , differentiate (23):

$$\ddot{I} = b\dot{S}I + bS\dot{I} = \left(bI \frac{dS}{dI} + bS \right) \dot{I} = (-bI + bS) \dot{I} \quad (24)$$

Thus two loops affect I , the reinforcing loop with strength $S_I(R) = bS$ and an effect which is balancing with absolute strength bI . However it is not clear that this behavior can be identified with $B1$, which is first order through S only. There are two ways this can be viewed:

1. There is an exogenous effect of the loop $B1$ on the inflow of I , rather like the situation in section 4.2.
2. There is second order loop between S and I which is hidden by the system dynamics notation of a conserved flow, as suggested by Mojtahedzadeh (2009b, figure 6a).

The second of these two is the preferred explanation, as the Bass model is a special case of the second order system where S and I have separate outflows (figure 17, equations 25–26) and $b = c$.

$$\dot{S} = -bSI \quad (25)$$

$$\dot{I} = cSI \quad (26)$$

The loop $B2$ is hidden by the conserved flow notation of system dynamics and only appears in figure 16 as a figure of eight through $R1$ and $B1$. Thus for I the loops are $S_I(R) = bS$ and $S_I(B2) = -bI$. The result is shifting loop dominance from R to $B2$ (figure 18), consistent

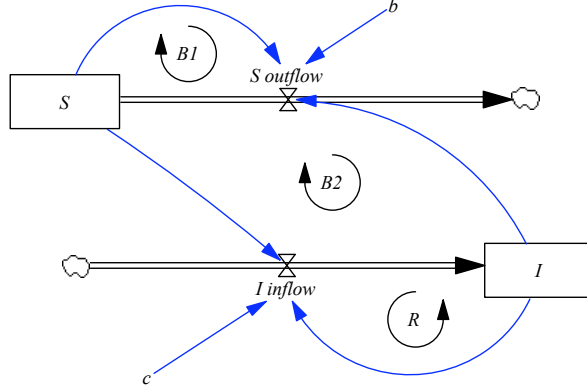


Fig. 17: Second Order Model that Reduces to Diffusion Model if $b = c$.

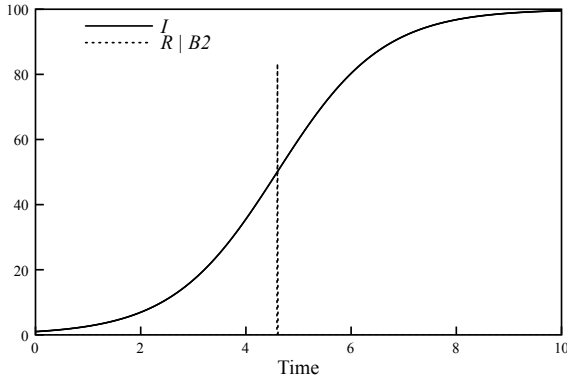


Fig. 18: Diffusion Model, Loop Dominance.

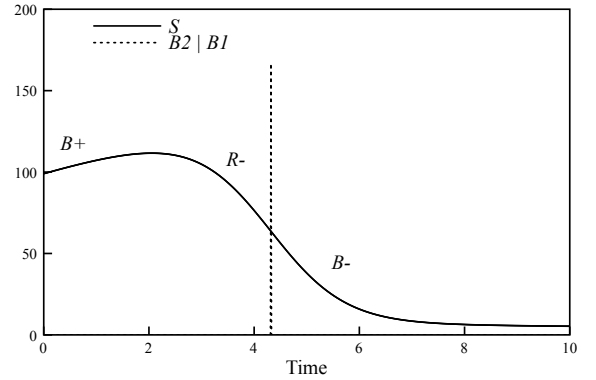


Fig. 19: Diffusion Model, Constant Inflow on S .

with the PPM analysis in Kampmann & Oliva (2011, figure 7). Note the Bass diffusion model has a similar explanation to the Limits to Growth model (section 3.2), as expected because the two models reduce to the same differential equation, the logistic equation.

For the variable S the two loops are both balancing, $S_S(B1) = -bI$ and $S_S(B2) = bS$. However the effect of $B2$ on S is *reinforcing* as S is decreasing, thus $B2$ is a flip loop. The addition of a constant inflow on S , $\dot{S} = a - bSI$ allows S to increase initially and for $B2$ to behave in the orthodox fashion as B^+ before changing to R^- when the net flow on S changes sign. Finally the behavior of S becomes B^- as loop dominance changes from $B2$ to $B1$ (figure 19).

In the 4 loop version of the diffusion model, figure 20, the loops are defined via an intermediate fraction or probability, S/N , where $N = S + I$ (e.g. Lyneis & Lyneis, 2006, figure 6; Mojtahedzadeh, 2011, figure 1c), often referred to as the standard incidence model (Hethcote, 1994). The equations now become:

$$\dot{S} = -b \frac{S}{N} I = -b \frac{S}{S+I} I \quad (27)$$

$$\dot{I} = b \frac{S}{N} I = b \frac{S}{S+I} I \quad (28)$$

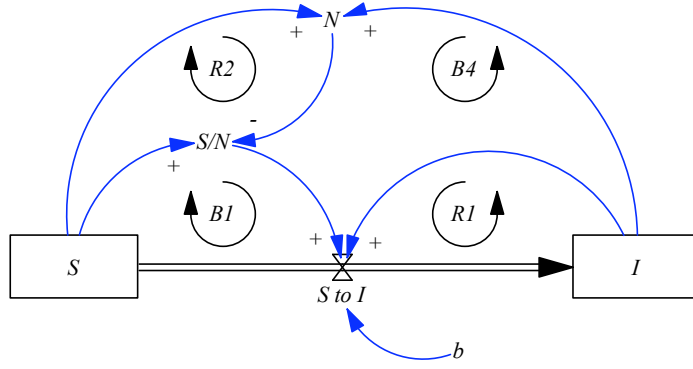


Fig. 20: Four Loop Diffusion, SD Model.

Two extra terms are generated for \dot{I} :

$$\dot{I} = \left(-b\frac{I}{N} + b\frac{S}{N} - b\frac{SI}{N^2} + b\frac{SI}{N^2} \right) I \quad (29)$$

There are now two additional loops, $B4$, and $R2$ (these are shown in a later model, figure 25). Lyneis & Lyneis (2006) describe these extra loops, whose strengths are the last two terms in (29), as dynamically inactive and self canceling, the latter confirmed by the terms being equal and opposite. Mojtahedzadeh (2011) applies the PPM method to this model using the software *Digest*, explicitly showing the equal and opposite contributions of the two loops (see Mojtahedzadeh, 2011, table 2, where *new reinforcing healthy loop* is $R2$ and *infected-healthy pathway* is $B4$). Thus these additional loops have no effect on either stock and they can be effectively excluded in a discussion of loop dominance. This is a direct consequence of the flow being conserved, $\dot{N} = 0$. The situation where the flow is not conserved will be considered under the SIR epidemic model (section 5.2).

5.2 SIR Epidemic Model

The SIR epidemic model is an extension of the diffusion model where the infected (actual customers) lose their infection and are no longer open to being infected again. Let S be the susceptibles, I the infected and R the removed. The model now has an extra balancing loop $B3$, compared with the diffusion model, figure 21, equations (30–32).

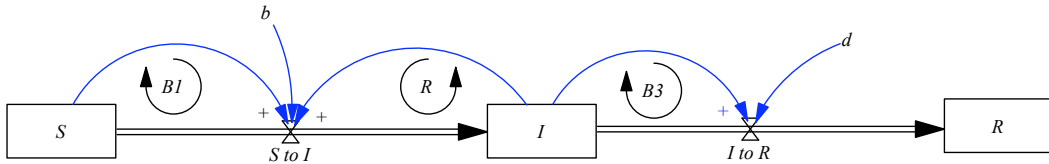


Fig. 21: SIR Epidemic, SD Model

$$\dot{S} = -bSI \quad (30)$$

$$\dot{I} = bSI - dI \quad (31)$$

$$\dot{R} = dI \quad (32)$$

To examine the effect of the loops on I , differentiate (31):

$$\begin{aligned}\ddot{I} &= b\dot{S}I + bSI - d = \left(bI \frac{dS}{dI} + bS - d \right) \dot{I} \\ &= \left(-\frac{b^2SI}{bS - d} + bS - d \right) \dot{I}\end{aligned}\quad (33)$$

Thus the strengths of the two first order loops are given by $S_I(R) = bS$, $S_I(B3) = -d$, and that of the hidden second order loop formed from the edges of R and $B1$ is $S_I(B2) = -b^2SI/(bS - d)$. The latter is a flip loop and changes sign as the epidemic passes through the threshold $S = d/b$.

Computing the loop strengths, and identifying dominant loops with the loop picker algorithm in an SD simulation, shows that the initial phase of behavior on I is reinforcing due to R (figure 22). At the inflection point dominance passes to $B2$ initially assisted by $B3$, reflected in the B^+ behavior, and eventually $B2$ on its own, showing the epidemic is slowing due to the restricted impact of the infected on a dwindling pool of susceptibles. At the threshold the flow dominance on I changes, and with it the polarity of $B2$. This loop now accelerates I 's decline with R^- behavior passing to a combination of R and $B2$. A second inflection point is passed leaving B^- behavior dominated by the draining process $B3$.

Thus the behavior of the infected can be split into four phases: accelerated growth through R , slowing growth through $B2$, accelerated decline through $B2$ having changed the polarity of its effect due to the change of flow dominance on I , and slowing decline through $B3$.

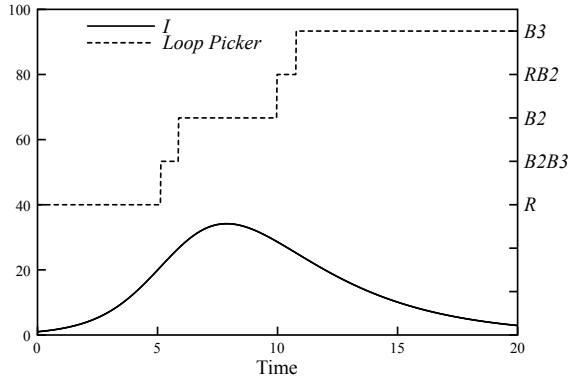


Fig. 22: Loop Dominance, SIR Model.

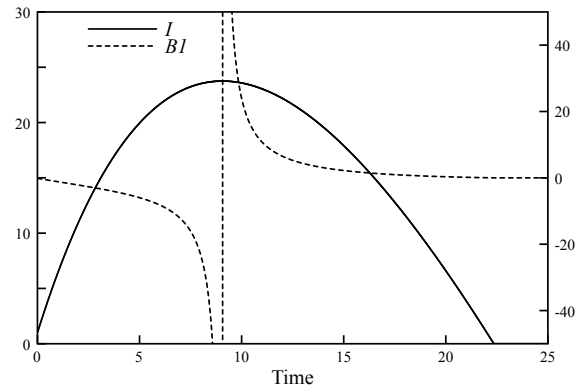


Fig. 23: Loop Strength, One Loop SIR Model.

The tipping point behavior of the SIR model is a result of a balancing loop changing polarity, i.e. a change of flow dominance, not a change of loop dominance as such. This can be seen by removing R and $B3$ from the model, as in figure 24.

The equations are now $\dot{S} = -bS$ and $\dot{I} = bS - d$. There are now no loops through I but $B1$ has an exogenous effect on I with strength $S_I(B1) = -bS/(bS - d)$. The effect flips polarity as the epidemic passes through the threshold, figure 23. As such it is *both* the loop structure *and* the flow structure that has determined the characteristic tipping point behavior of an epidemic.

Returning to the four loop version of the diffusion process, consider an epidemic where the disease results in death, figure 25, equations (34–36).

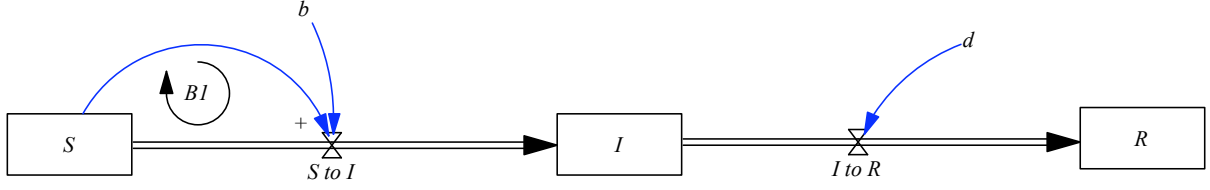


Fig. 24: Cut down SIR model to Illustrate Tipping Point Behavior.

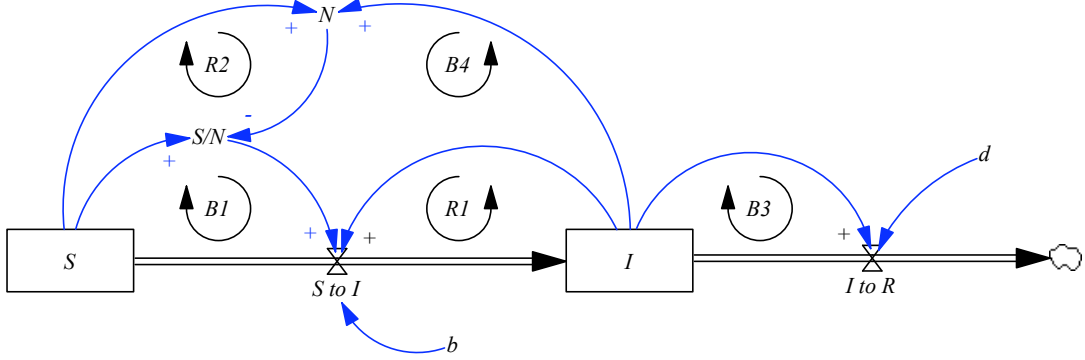


Fig. 25: SIR Standard Incidence Model with Deaths, $N = S + I$.

$$\dot{S} = -b\frac{S}{N}I \quad (34)$$

$$\dot{I} = b\frac{S}{N}I - dI \quad (35)$$

$$\dot{R} = dI \quad (36)$$

Unlike the four loop Bass diffusion model $N = S + I$ is no longer constant, $\dot{N} \neq 0$, and the loops $B4$ and $R2$ will no longer be self canceling. Differentiating equation (35), gives, after some algebra:

$$\ddot{I} = \left(\frac{bS}{N} - \frac{b^2SI}{bS - dN} - d - \frac{bSI}{n^2} + \frac{b^2S^2I}{n^2(bS - dN)} \right) \dot{I} \quad (37)$$

where the loop strengths of $R1$, $B2$, $B3$, $B4$ and $R2$ are given by the consecutive terms in the brackets of (37)³. By comparing the loop strengths in an SD simulation the different phases of loop dominance on I can be identified using the loop picker, figure 26 and table 1. Although the many changes of structural dominance look complex, from a behavioral point of view there are still only four phases:

1. R^+ , where $R1$ dominates, latterly assisted by $R2$;
2. B^+ , where the second order $B2$ dominates with negative effect on I , initially assisted by combinations of $B3$ and $B4$;
3. R^- , where $B2$ remains dominant, but now with positive effect on I , assisted latterly by $R1$;

³Strictly speaking it is not $R2$ that is through I but a hidden second order loop formed from it, in a similar way that $B2$ is formed using edges from $R1$ and $B1$.

4. B^- , where $B3$ dominates, initially assisted by combinations of the flip loop $R2$ (which now has negative effect) and $B4$.

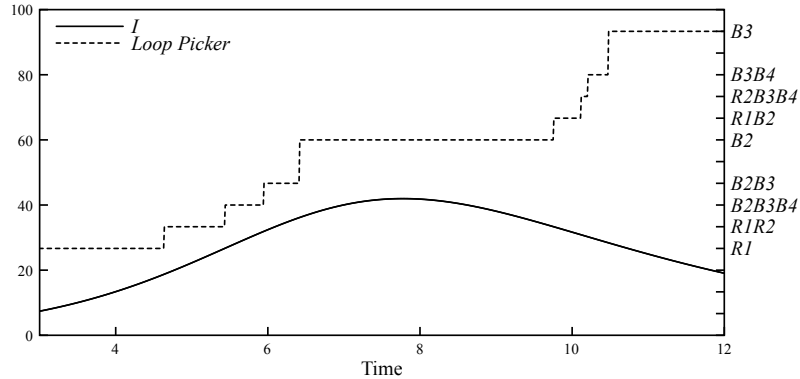


Fig. 26: Loop Dominance, Four Loop SIR Model.

Start Time	0.0	4.7	5.5	6.0	6.5	9.8	10.2	10.3	10.5
Loops through I	$R1$	$R1R2$	$B2B3B4$	$B2B3$	$B2$	$R1B2$	$R2B3B4$	$B3B4$	$B3$
Behavior of I	R^+		B^+			R^-		B^-	

Table 1: Change of Loop Dominance, Four Loop SIR Model.

Thus despite the two additional loops, which no longer self cancel, the fundamental explanation of the behavior of I in terms of the loops, $R1$, $B2$ and $B3$ is the same as the two loop SIR model as the additional loops are relatively weak.

6 A Practical Method for Stella⁴ Models

6.1 Outline of Method

Comparing the effects of different loops and structures on a stock is clearly a helpful way of understanding the behavior of that stock. However the preceding analytical approach, which requires the use of calculus to compute the loop strengths, will place the method beyond the reach of many system dynamicists who are more comfortable with stock/flow diagrams and simulation. Although there are specialist tools for identifying loop strengths (e.g. Mojtahedzadeh et.al., 2004), for the method to be practical it needs to be implemented easily into standard SD simulation software, similar to those proposed by Kim (1995), Ford (1999) and Myrtveit & Saleh (2000). This section describes such an implementation in Stella, applied to the yeast model (Saleh, 2002) for comparison with previous studies.

The computation of the loop strength requires the derivative of the last element in each loop prior to it entering the flows of the nominated stock. In outline the method is:

⁴In principle the method should work in any SD simulator that has arrays with pre-defined array functions.

1. Ensure each loop has a converter prior to its entry to the flow of each stock x . This is used to identify the loops whose edges are combined by multiplication. This is the “loop identifier converter” L .
2. Determine the derivative of the stock x with respect to time t , using the difference between the inflow and the outflow, dx/dt .
3. Use the loop identifier converter to compute its derivative with respect to t and divide by the t derivative of x from [2], i.e. $dL/dx \div dx/dt$ (chain rule of differentiation) to give differentiation of the loop identifier by x . Where two loop identifiers are multiplied L_1L_2 , the loop strength of L_1 , for example, is the derivative of L_1 multiplied by L_2 (from the product rule of differentiation).
4. Check a table of loop strengths to determine which loops change the sign of their effect on the stock, i.e. the flip loops.
5. Determine all possible combinations of reinforcing loops, and of balancing loops, bearing in mind that flip loops will be in both. Use the information to set the element names of an array dimension.
6. Place the loops strengths in an array with the appropriate element name. The loop picker algorithm, described in the appendix, uses a combination of arrays to identify the loop, or loop combination, which is larger than the sum of all the loops of the opposite polarity. This is the loop/loop combination that is deemed to explain the behavior of the stock, specifically its change and its curvature.

6.2 The Yeast Model

The yeast model is a simple second order model of overshoot and decline that is one of a number useful benchmarks for the analysis of loop dominance (Saleh, 2002; Guneralp, 2005; Phaff, 2006; Huang, 2009; Mojtahedzadeh, 2009a). The model is taken from the details given by Huang (2009). The effect of the loops on the stock **Cells**, C , are investigated.

1. Construct the model with loop identifier converters prior to entry to the flows of the stock, figure 27, e.g. **R_loop**. There are four loops: R and $B1$ are first order, with $B2$ and $B3$ second order. The converters normally connected to the flow, e.g. division time, are connected to one of the incoming loop identifiers.
2. Determine the time derivative of the stock as the difference of its inflow and outflow, **dC_by_dt** in figure 28.
3. Compute the derivative of the loop identifier converter with respect to the stock C by computing its time derivative and using the chain rule. For example **R_strength** = **B2_loop*DERIVN(R_loop,1)/dC_by_dt**, figure 28. The multiplication by **B2_loop** is a result of the product of the two loops. Loop strengths from the outflows require a minus sign to achieve the correct polarity.
4. Check a table of loop strengths to identify which loops flip polarity, table 2. It is noted $B2$ and $B3$ both change polarity at the maximum of **Cells**. As flips loops they will

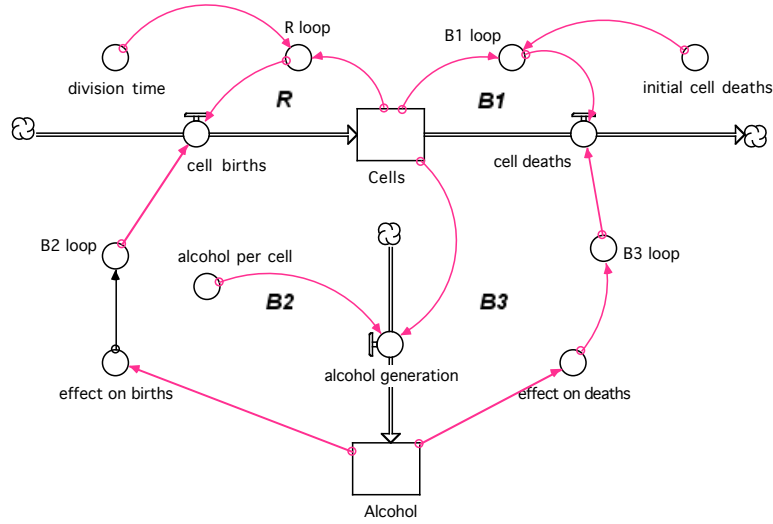


Fig. 27: Yeast Model with Converters Added to Identify Loops.

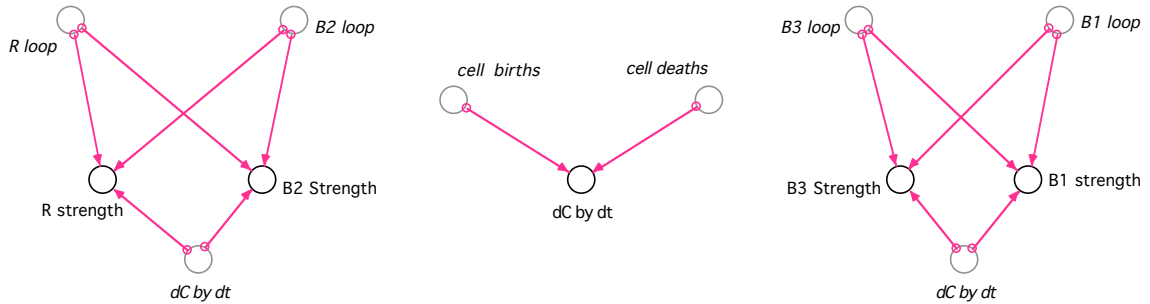


Fig. 28: Computing Loop Strengths in the Yeast Model.

need to be combined with R as well as $B1$, but only when their polarities match. It is noted that R also changes polarity towards the end of the simulation. This is due to `effect_on_births` becoming negative, thus making the inflow negative. However as the flow is a uniflow this loop does not flip polarity and does not need to be combined with $B1$.

Time	Cells	R strength	$B1$ strength	$B2$ strength	$B3$ strength
65.40	39.86	9.63e-03	-9.14e-03	-5.70	-7.33
65.45	39.86	1.06e-02	-1.04e-02	-16.61	-21.77
65.50	39.86	6.95e-03	-7.07e-03	17.81	23.81
65.55	39.86	8.05e-03	-8.49e-03	5.75	7.84

Table 2: Change of Polarity of the Effect of $B2$ and $B3$ on Cells (in bold).

5. Compute all possible combinations of loops. The reinforcing combinations are: $RB2$, $RB3$ and $RB2B3$, with the balancing ones $B1B2$, $B1B3$ and $B1B2B3$. Thus ten dimension element names are required when the four single loops are also considered. The dimension is named `cell_loops` and, for example, the element where the $RB2$ combination is to be stored is called `RB2dimension`.
6. Use the loop picker algorithm to identify the dominant loops. The details of the algorithm are in the appendix. Most steps are automated, such as the identification of

loop type, the sum of reinforcing and balancing loops. The `single_loops` converter requires the loop strengths assigned to the appropriate element, with all the combination elements set to zero, figure 35. The `loop_combinations` converter is set with the appropriate combinations, conditional on the loops being reinforcing or balancing. The `valid_combination_codes` converter identifies the number of loops in each combination. The converters `loop_picker` and `change_of_dominance` contain the details of change of the dominant loop/loop combinations.

The results are given in figure 29 and table 3. There are four main phases of loop dominance. Growth starts with R^+ behavior due to loop R . The second main phase is B^+ dominated by $B2$. However at the start of this phase, time 50.85, there is a brief period where it takes $B1$, $B2$ and $B3$ together to dominate over R . This result has been checked by analytic differentiation. The period is brief because $B1$ and $B3$ are very weak at this stage.

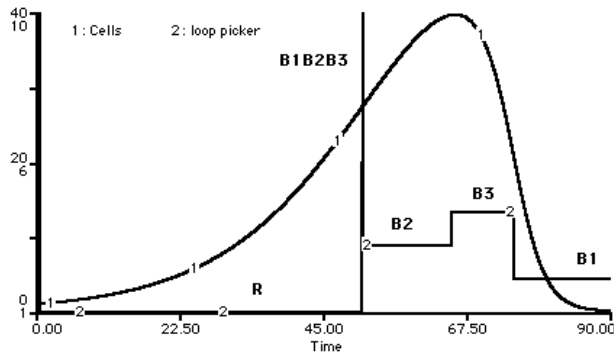


Fig. 29: Loop Dominance, Yeast Model.

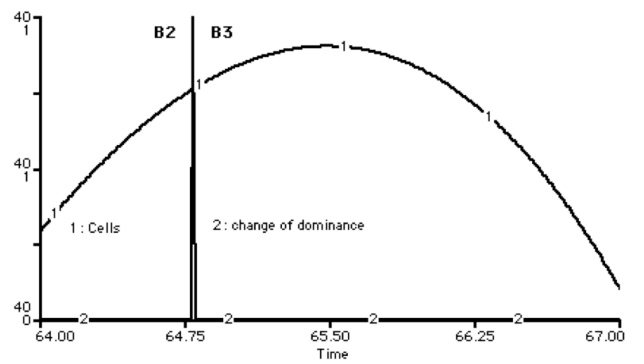


Fig. 30: B2 B3 Transition, Yeast Model.

Start Time	0.00	50.85	50.90	64.80	65.50	74.75
Loops through Cells	$R1$	$B1B2B3$	$B2$	$B3$	$B1$	
Behavior of Cells	R^+	B^+			R^-	B^-

Table 3: Change of Loop Dominance, Yeast Model.

The third main phase is where $B3$ dominates, time 64.80, table 3. Interestingly this change of dominance occurs before the peak, the point where the polarity of $B2$ and $B3$ change, time 65.50, and the behavior changes to R^- , figure 30. As in earlier models this confirms that the turning point is not caused by a change of loop dominance but by a change of loop polarity due to the change of flow dominance on Cells. Indeed it only takes the presence of one of the loops $B2$ and $B3$ to produce the behavior of this model (Mojtahedzadeh, 2009a). The effect of $B3$ is now positive, hence the accelerating decline in this phase.

The final phase is where the behavior is B^- and the draining process $B1$ dominates. Thus the implementation of the numerical method in Stella has correctly picked up the changes in loop dominance, as measured by the different pathways that explain the changes in the curvature of the stock Cells in terms of its net flow.

6.3 Market Growth Model

For a second illustration of the method consider Forrester’s (1968b) market growth model which demonstrates internal limits to growth due to a firm’s inability to satisfy customer delivery expectations (Morecroft, 1983). Using the version given in Sterman (2000, Ch. 15) there are four major loops through the the stock *Backlog*, *R1* the sales growth, *B1* the order fulfillment, *B2* the capacity expansion, and *B3* the customers’ response to product availability affected by delivery delays (figure 31). In order to use the loop picker algorithm on *Backlog* a fifth loop needs to be considered for the utilization of capacity, *R2*, as in Sterman’s version of the model *Capacity* determines the shipment rate indirectly through *Capacity Utilization* as well as the direct link.

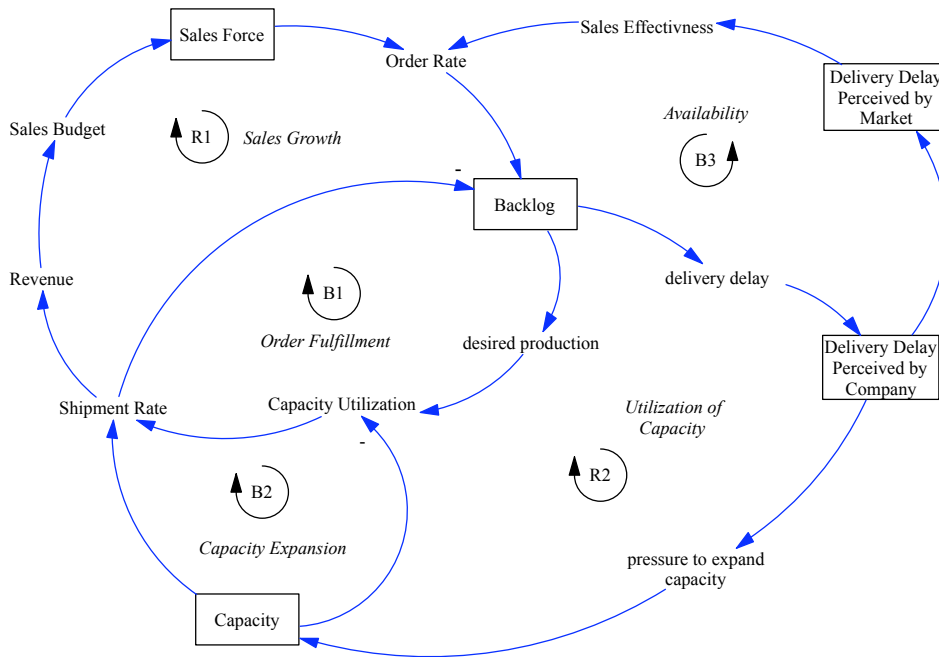


Fig. 31: Market Growth Model (all links positive unless indicated otherwise).

The model in Stella was taken from the CD that accompanies Sterman’s book; the links to *Backlog* given in figure 32. As there are five such links, and all but one belong to higher order loops and could thus potentially flip, then all 31 combinations of the loops are considered. *Sales Force* and *Sales Effectiveness* are multiplied, thus loop identifiers are placed in each branch and the product placed in a separate converter, *sales and availability multiply*, so that each branch can be identified for the product rule (figure 33).

The outflow of *Backlog* is more complicated as *R2* and *B1* combine in *Capacity Utilization* prior to being combined with *Capacity*, and thus share a common edge to *Shipment Rate* (figure 32). In order to separate the strengths of the two loops, loop identifiers are placed prior to their combination in *Capacity Utilization*, and a combined loop identifier placed in the common edge (figure 33). This will enable the chain rule of partial differentiation to combine the change across the common edge with each change across the individual paths of both *R2* and *B1*. The combination of the two edges in *Capacity Utilization* (combined by division), is separated from the graphical converter, referred to as *desired over capacity*. Additionally the graphical converter is replaced by a continuous formula, obtained by fitting

a cubic spline to the reference points, as the discrete nature of a graphical converter can cause discontinuities in the numerical differentiation.

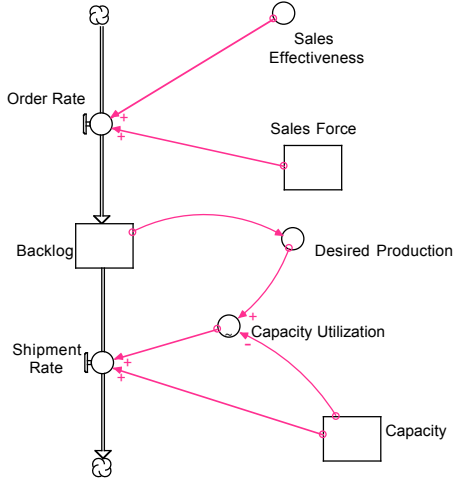


Fig. 32: *Backlog*, Sterman's Original Model

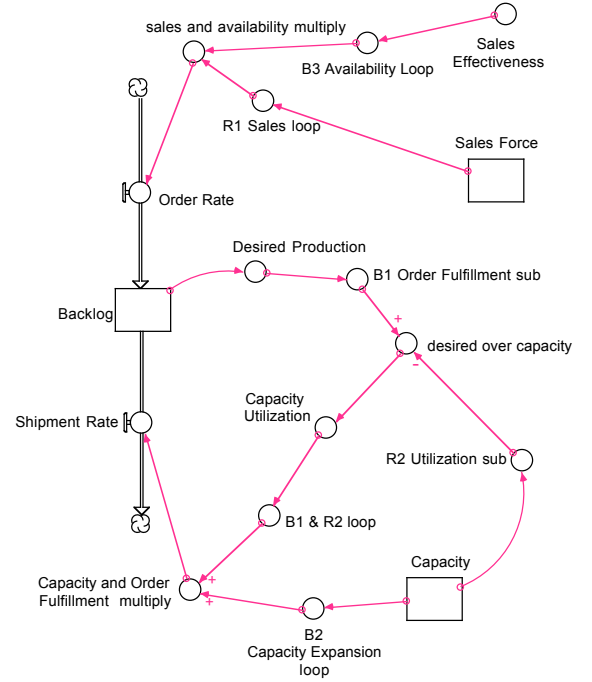


Fig. 33: *Backlog*, Loop Identifiers Added

The loop strengths for $R1$, $B2$ and $B3$ are computed in a similar way to the Yeast model. For $B1$ the loop strength requires the change in the common loop identify $B1 \& R2$ loop, with respect to the formula in the common edge, *desired over capacity*, multiplied by the change in the identifier for $B1$, $B1$ sub, with respect to the backlog (38).

$$S_{backlog}(B1) = \frac{\partial B1R2 \text{ loop}}{\partial \text{formula}} \times \frac{\partial B1 \text{ sub}}{\partial \text{backlog}} \quad (38)$$

The implementation of these rules in Stella is given by:

```

B1_order_fulfillment_strength =
  change_on_combined_order_util*(1/R2_Utilisation_sub)
  *DERIVN(B1_order__fulfillment_sub,1)/d_backlog_by_dt
change_on_combined_order_util =
  -B2_capacity_loop*DERIVN(B1_&_R2_loop,1)
  /(DERIVN(desired_over_capacity,1)+very_small)

```

Again the partial derivatives of the dependent variables have been estimated by comparing their time derivatives. Note the $1/R2_Utilisation_sub$ reflects the quotient in the formula in *desired over capacity*. The minus sign is because the loop is connected to the outflow. The strength of $R2$ is handled in a similar fashion.

Applying the loop picker algorithm to the model, with Sterman's parameter values, identifies the loop combinations for *Backlog*, figure 34. From about 25 months onwards sales $R1$ drives the growth, with availability $B3$ causing the turn around in the backlog as customers leave in response to long delivery delay times. Eventually the capacity expansion loop $B2$ takes over the role of reducing the backlog, but it is always too late to prevent customers leaving.

Thus capacity expansion only plays a minor role in reducing backlogs and is never the major reason for the turn around in backlog which is in the hands of the customers, as intended by the model. Note there is brief period where the order fulfillment loop $B1$ dominates prior to the customers returning, with $B3$ being responsible for the backlog increasing again.

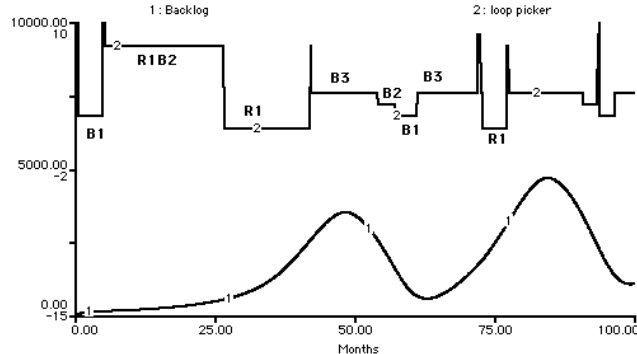


Fig. 34: Loop Dominance for *Backlog* in Market Growth Model.

Although beyond the scope of this paper, policies can be applied to reduce the period where product availability reduces the backlog and increase the period dominated by capacity expansion. It can be shown how difficult this is to achieve by changing parameter values alone. Thus a knowledge of loop dominance can bring insights into the effect of policy changes in terms of the underlying causes and structure ⁵.

It should be noted that in the early period, growth in the backlog occurs because of a combination of sales, $R1$, and capacity reduction, $B2$, figure 34. This is due to *Capacity*'s initial value being too high for this scenario. Reducing its initial value can remove this phase and give a more realistic scenario for a new company.

7 Conclusion

This paper has shown that comparing the strengths of the causal loops has given a quantitative explanation for model behavior in terms of its loop and flow structure. Following the pathway participation metric (PPM) method, loop strength is defined in terms of the effect of a change in net flow (first derivative) on the curvature (second derivative) of a given stock. For simple systems those loops strengths can be examined analytically and the results used to enhance a simulation in order to promote understanding of the behavior in terms of structure. In addition to confirming well known results, such as shifting loop dominance, examining loop strengths has been able to uncover the complex loop interpretation of the SIR model, showing that additional loops have little effect on the solution, and the importance of external loop structures on a system. It is hoped the paper will encourage others to derive loop strengths of small models in order to provide some additional analysis and understanding.

In addition the paper has presented a numerical method for deriving loop strengths in a propriety SD simulator, such as Stella. The algorithm may be copied from the file in the

⁵The market growth model in Stella with the loop picker algorithm is available on request.

supporting materials, and with small modifications be applied to one or more stocks in a model⁶. An analysis of the loops of the Yeast Model has matched previous studies. The numerical method has been applied to all the models analyzed in the earlier sections and the results match the analytical computations.

Although much of the loop picker algorithm is automated there is some manual work required to apply the method to each stock. If an analysis of the effect of the loops on every stock in a model is required then the method may become too time-consuming to implement if there are many stocks. Nevertheless if not all stocks are required then model size should not be a major limitation.

However model complexity is a more serious issue. Because this method uses a specific definition of loop strength based on PPM, all the latter's limitations will apply, such as: difficulty with graphical converters; no natural explanation of delays and the complicated handling of oscillations (Kampmann & Oliva, 2011). At present the numerical method has only been used on additive, multiplicative, and division flow algebra. Other combinations will require more rules, or could be handled by breaking converters down into basic algebraic steps. Finally the method as stated has only been applied to stocks, although some transformations should enable the strength of a loop on an auxiliary to be computed. Further work is needed to determine to what extent model complexity will limit the use of the method in an SD simulator.

It is unlikely that any one method of quantifying structure can be applicable to all types of models or behaviors. However the advantage of the numerical approach, proposed within this paper, is that it will enable a system dynamicist to gain structural insights into their model behavior within an SD simulator, without the need for specialist software or mathematics. As such it is hoped it will widen interest in a quantitative understanding of loop and structure behavior.

References

- Ford DN. (1999). A behavioural approach to feedback loop dominance analysis. *System Dynamics Review*, **15:1**, 3–36.
- Forrester JW. (1968a). *Principles of Systems*. Peagamus Communications, Waltham MA.
- Forrester JW. (1968b). Market growth as influenced by capital investment, *Industrial Management Review*, **9:2**, 83–105.
- Guneralp BG. (2005). Progress in eigenvalue elasticity analysis as a coherent loop dominance analysis tool. *Proceedings of the 23rd International Conference of the System Dynamics Society*, Boston, USA, The System Dynamics Society.
- Hethcote HW. (1994). A thousand and one epidemic models. In *Frontiers in Mathematical Biology*, Levin SA (ed). Berlin: Springer Verlag.
- Huang J, Howley E and Duggan J. (2009). The Ford Method: A sensitivity analysis approach. *Proceedings of the 27th International Conference of the System Dynamics Society*, Albuquerque, USA, The System Dynamics Society.

⁶Other models with the loop picker algorithm are available from the author by email

- Kampmann CE. (1996). Feedback loop gains and system behavior. *Proceedings of the 14th International Conference of the System Dynamics Society*, Cambridge, MA, USA, The System Dynamics Society.
- Kampmann CE and Oliva R. (2011). System dynamics, analytical methods for structural dominance, analysis in. In *Complex Systems in Finance and Econometrics*, Meyers RA (ed). Springer, 833–852.
- Kim D. (1995). A new approach for finding dominant feedback loops: Loop by loop simulation for tracking feedback loop gains, *Proceedings of the 13th International Conference of the System Dynamics Society*, Tokyo, Japan, The System Dynamics Society.
- Lyneis JM and Lyneis DA. (2006). Three loops, or four loops: Pedagogic issues in explaining basic epidemic dynamics, *Proceedings of the 24th International Conference of the System Dynamics Society*, Nijmegen, The Netherlands, The System Dynamics Society.
- Mojtahedzadeh M. (2009a). Do parallel lines meet? How can pathway participation metrics and eigenvalue analysis produce similar results? *System Dynamics Review*, **24:4**, 451–478.
- Mojtahedzadeh M. (2009b). Objective analysis of subjective feedback structures: The problem of consistency in explaining model behavior, *Proceedings of the 27th International Conference of the System Dynamics Society*, Albuquerque, USA, The System Dynamics Society.
- Mojtahedzadeh M. (2011). Consistency in explaining model behavior based on its feedback structure, *System Dynamics Review*, **27:4**, 358–373.
- Mojtahedzadeh M, Anderson D and Richardson GP. (2004). Using *Digest* to implement the pathway participation method for detecting influential system structure, *System Dynamics Review*, **20:1**, 1–20.
- Mojtahedzadeh M and Richardson GP. (1995). Confusion in the polarity of major loops, *Proceedings of the 13th International Conference of the System Dynamics Society*, Tokyo, Japan, The System Dynamics Society.
- Morecroft J. (1983). System Dynamics: Portraying bounded rationality, *Omega*, **11:2**, 131–142.
- Myrtveit M and Saleh M. (2000). Superimposing dynamic behavior on causal loop diagrams of system dynamic models. *Proceedings of the 18th International Conference of the System Dynamics Society*, Bergen, Norway, The System Dynamics Society.
- Phaff HWG. (2008). Generalized loop deactivation method. *Proceedings of the 26th International Conference of the System Dynamics Society*, Athens, Greece, The System Dynamics Society.
- Phaff HWG, Slinger JH, Guneralp B and van Daalen CE. (2006). Investigating model behavioral analysis: A critical examination of two methods, *Proceedings of the 24th International Conference of the System Dynamics Society*, Nijmegen, The Netherlands, The System Dynamics Society.

- Richardson GP. (1986) [1976]. Problems with causal loop diagrams, *System Dynamics Review*, **2:2**, 158–170.
- Richardson GP. (1995)[1984]. Loop polarity, loop dominance, and the concept of dominant polarity, *System Dynamics Review*, **11:1**, 67–88. First appeared in *Proceedings of the 2nd International Conference of the System Dynamics Society*, Oslo, Norway, The System Dynamics Society.
- Richardson GP. (1997). Problems in causal loop diagrams revisited, *System Dynamics Review*, **13:3**, 247–252.
- Richardson GP. (2011). Reflections on the foundations of system dynamics. *System Dynamics Review*, **27:3**, 219–243.
- Saleh MM. (2002). *The Characterization of Model Behavior and its Causal Foundation*. PhD Dissertation, University of Bergen, Bergen, Norway.
- Saleh MM and Davidsen PI. (2000). An eigenvalue approach to feedback loop dominance analysis in non-linear dynamic models. *Proceedings of the 18th International Conference of the System Dynamics Society*, Bergen, Norway, The System Dynamics Society.
- Sterman JD. (2000). *Business Dynamics: Systems Thinking and Modeling for a Complex World*, McGraw Hill.

Appendix - Loop Picker Algorithm

The purpose of the algorithm is to compute the largest loop, or loop combination, strength for the smallest set of loops, that dominates the total of all the loops of the opposite polarity. For example if a system is in reinforcing behavior it is found that $R1$ together with $R2$ dominate the algorithm will exclude the combination $R1R2R3$ as it is a larger set. It would also exclude $R1R3$ if it is smaller than $R1R2$, and also exclude the individual loops if they are not sufficient on their own to dominate. Additionally the algorithm takes into account the possible change of polarity of loops. Although Stella has no iteration (for loops) in its programming, the algorithm can be achieved with arrays and built-in functions alone.

All converters referred to are displayed in figure 35. They are described for a generic stock x .

1. Construct an array dimension for each stock, e.g. `x_loops`. The array index should be labeled with the name of each loop into the stock, e.g. `B2dim`, and all viable combinations, taking into account loops that change polarity, e.g. `B1B2dim`.
2. Place all the loop strengths in an array, matching the strength with the dimension name: `single_loops`. E.g. `single_loops[B2dim]=B2_Strength`. Combinations of loops should set as zero initially.
3. Construct an array `loop_type` parallel to `single_loops` to identify the type of loop, using $(S(L) - |S(L)|)/(2S(L))$. Reinforcing loops are labeled 1, and balancing loops are labeled 0. This formula will pick up a change of loop polarity, adding a very small number `very_small` in the denominator to prevent zero divide

```

loop_type = (single_loops[x_loops] + abs(single_loops[x_loops]))
            / (2*single_loops[x_loops]+very_small)

```

4. Use the loop type array with the single loops array to have one array of reinforcing loops only, and one of balancing loops only.

```

R_loops = loop_type[x_loops]*single_loops[x_loops]
B_loops = single_loops[x_loops]*(1-loop_type[x_loops])

```

5. Use `R_loops` and `B_loops` to create converters for the sum of reinforcing loops, `sum_of_R_loops`, and all balancing loops `sum_of_B_loops`. E.g. `R_loops = ARRAYSUM(R_loops[*])`. The sum which is the greater will indicate whether the behavior of x is in reinforcing or balancing mode.
6. Construct an array to contain the strengths of all the loops *and* the loop combinations. The single loops are unchanged from `single_loops`, but the combinations now contain appropriate sums of loops. If a loop can change polarity then the combination should only take place if the loops are of the same polarity, otherwise it is set zero. Thus the combination will only be counted when the loops agree on polarity.

```

loop_combinations[B2dim] = single_loops[B2dim]
loop_combinations[B1B2dim] =
    if (loop_type[B2dim]<0.5)
        then (single_loops[B1dim]+single_loops[B2dim])
        else (0)

```

The restriction “< 0.5” represents “= 0”, for balancing loops, but takes into account small variations from 0 due to the small number in the numerator of the `loop_type` formula that fixed the zero divide. Likewise “= 1” for reinforcing loops needs to be “> 0.5”.

7. The `loop_type` formula was only valid for single loops. It now must be redefined to include all loop combinations, again with a very small number to avoid the zero divide:

```

revised_loop_type
= (loop_combinations[x_loops] + abs(loop_combinations[x_loops]))
  / (2* loop_combinations[x_loops]+very_small)

```

This formula will identify changes of polarity in a loop/loop combination.

8. Construct an array which subtracts from each loop and loop combination the sum of the loops of opposite polarity. Thus only loops and loop combinations which are greater than the total opposing loops are positive. These are dominant, but some may be constrained as subsets of larger combinations. Divide by the sum of all the loops to give a relative number, thus the largest possible value in this array is 1.

```

dominant_search[x_loops] =
    (abs(loop_combinations[x_loops])
     -(1-revised_loop_type[x_loops])*sum_of_R_loops
     -revised_loop_type[x_loops]*sum_of_B_loops)
    / (sum_of_R_loops+sum_of_B_loops+very_small)

```

Again a correction to prevent zero divide is needed.

- Construct an array `combination_code` coded to indicate how many loops are in a given combination, e.g. single loops are coded 1, two loops combined are coded 2, etc. Combine this with `dominant_search` to ensure that only codes of dominant loop/loop combinations remain.

```

valid_combination_codes[x_loops] =
  if(dominant_search[x_loops]>0)
    then(combination_code[x_loops])
    else (100)

```

This array will contain the number of loops in the dominant combinations. The non-dominant ones are set to a number bigger than the maximum possible of combinations likely to be used in a model, in this case 100.

- Compute the minimum combination code `ARRAYMIN(valid_combination_codes[*])`. The dominant loop/loop combination will be of this number of loops. Any larger combinations, although dominating, will not be the minimum possible number to exceed the sum of the opposing loops.
- All dominant loops with a larger combinations of loops than are required are removed by setting them at a number smaller than 0, e.g. -1.

```

dominant_loops[x_loops] =
  if(minimum_valid_combination_code = valid_combination_codes[x_loops])
    then (dominant_search[x_loops])
    else (-1)

```

- The `loop_picker` is a converter to select the index of the largest of the remaining dominant loop/loop combinations, using `ARRAYMAXIDX(dominant_loops[*])`. This can be plotted with x or tabulated to indicate which loop/loop combination is dominant in the behavior of x at any time, e.g. figure 29.
- Finally the times at which dominance changes can be marked out by comparing the loop picker value with the one at the previous time step and checking for changes.

```

change_of_dominance =
  if (abs(loop_picker-delay(loop_picker,DT)) >small_for_equality )
    then (1)
    else (0)

```

Because equality is not well defined for floating point numbers a small number, `small_for_equality` is needed to test the absolute value of the difference of the two items. DT may need to be adjusted to fine-tune this part of the algorithm. The change of dominance can also be plotted with x , to mark the different phases of dominance, e.g. figure 30.

The full code is available in the supplementary file or will be sent on request.

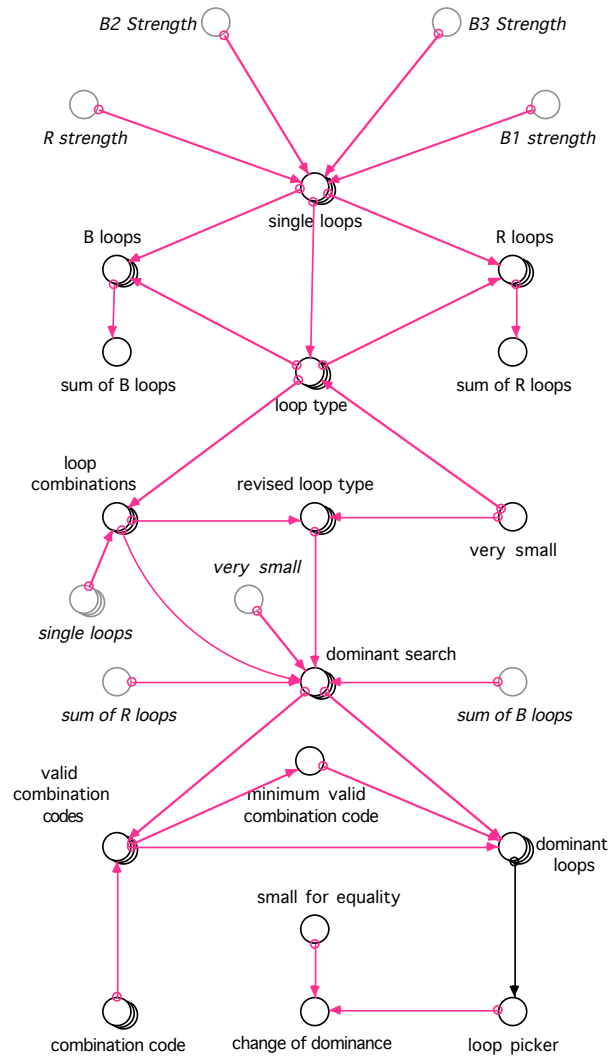


Fig. 35: Loop Picker Algorithm in Stella.